microbial biotechnology

Open Access

Repurposing the FDA-approved anticancer agent ponatinib as a fluconazole potentiator by suppression of multidrug efflux and Pma1 expression in a broad spectrum of yeast species

Lin Liu,[1,†] Tong Jiang,[2,3,†] Jia Zhou,[1] Yikun Mei,[1] Jinyang Li,[1] Jingcong Tan,[1] Luqi Wei,[1] Jingquan Li,[1] Yibing Peng,[4,5] Changbin Chen,[2,6,*] Ning-Ning Liu[1,**] and Hui Wang[1,*]**

[1]*State Key Laboratory of Oncogenes and Related Genes, Center for Single-Cell Omics, School of Public Health, Shanghai Jiao Tong University School of Medicine, Shanghai, 200025, China.*

[2]*Center for Microbes, Development and Health, Key Laboratory of Molecular Virology and Immunology, Institut Pasteur of Shanghai, Chinese Academy of Sciences, Shanghai, 200031, China.*

[3]*University of Chinese Academy of Sciences, Beijing, China.*

[4]*Department of Laboratory Medicine, Ruijin Hospital, Shanghai Jiao Tong University School of Medicine, No. 197 Ruijin ER Road, Shanghai, 200025, China.*

[5]*Faculty of Medical Laboratory Science, Shanghai Jiao Tong University School of Medicine, No. 197 Ruijin ER Road, Shanghai, 200025, China.*

[6]*The Nanjing Unicorn Academy of Innovation, Institut Pasteur of Shanghai, Chinese Academy of Sciences, Nanjing, 211135, China.*

Summary

Fungal infections have emerged as a major global threat to human health because of the increasing incidence and mortality rates every year. The emergence of drug resistance and limited arsenal of antifungal agents further aggravates the current situation resulting in a growing challenge in medical mycology. Here, we identified that ponatinib, an FDA-approved antitumour drug, significantly enhanced the activity of the azole fluconazole, the most widely used antifungal drug. Further detailed investigation of ponatinib revealed that its combination with fluconazole displayed broad-spectrum synergistic interactions against a variety of human fungal pathogens such as *Candida albicans*, *Saccharomyces cerevisiae* and *Cryptococcus neoformans*. Mechanistic insights into the mode of action unravelled that ponatinib reduced the efflux of fluconazole via Pdr5 and suppressed the expression of the proton pump, Pma1. Taken together, our study identifies ponatinib as a novel antifungal that enhances drug activity of fluconazole against diverse fungal pathogens.

Received 27 November, 2020; revised 23 March, 2021; accepted 24 March, 2021.

For correspondence. *E-mail huiwang@shsmu.edu.cn; **E-mail liuningning@shsmu.edu.cn; ***E-mail cbchen@ips.ac.cn

[†]Co-first author.

Microbial Biotechnology (2022) **15**(2), 482–498
doi:10.1111/1751-7915.13814

Introduction

Combinatorial therapy with commercially available drugs has been becoming an effective strategy to address the rising concern of the limited arsenal of antifungals coupled with the growing number of drug-resistant clinical isolates and to satisfy the ever-increasing clinical requirements (Mishra *et al*., 2007; Ruggero and Topal, 2014). Currently available antifungals could be usually classified into following three major categories: polyenes, echinocandins and azoles (Shapiro *et al*., 2011). Polyenes with antifungal activities were discovered and developed more than 60 years ago, and the molecules were found to inhibit fungal growth by binding to the ergosterol components in the plasma membrane (Anderson *et al*., 2014). However, translational research has shown that polyenes, which are mainly excreted from urine and bile, are able to cause severe nephrotoxicity and hepatotoxicity, and thus greatly limit their clinical applications (Gray *et al*., 2012). Echinocandins were introduced over 10 years ago, and the compounds were appreciated by its ability to inhibit the synthesis of (1, 3)-β-glucan, a major component of fungal cell wall (Shekhar-Guturja *et al*., 2016b). Although echinocandins have been recognized as one of today's best-studied non-ribosomal peptide natural product families, problems still exist, especially a very low level of oral bioavailability and a short half-life. Azoles, known as the most widely used antifungal agents, have been used in clinic for more than 40 years (Shapiro *et al*., 2011). The azole-based drugs

were identified to effectively inactivate the ergosterol synthase (cytochrome P_{450}) and block ergosterol synthesis, resulting in the accumulation of C-14 methyl sterol (Shekhar-Guturja *et al*., 2016b). As for the potential side-effect of this drug family, studies have shown that metabolized azoles in the liver are mainly excreted from bile which easily results in hepatotoxicity.

Notably, the development of new antifungal turns out to be expensive, laborious and time-consuming and cannot be relied on during the recurrent and emerging challenge of fungal infections. For example, it took nearly 30 years for echinocandins, the most recent class of antifungals, to develop and obtain success from bench to bedside (Basso *et al*., 2020). There is a pressing need to develop new antifungal therapeutic agents, and recent studies have strongly suggested that drug repurposing provides an attractive solution for antifungal development, with apparent advantages including the validated information about the knowledge base for the pharmacokinetics and pharmacodynamics, a dramatic shortening of the Research & Development (R&D) cycle and the huge cut of the R&D costs to achieve maximal utilization of the medical resources. There have been several examples of development of new antifungals based on this strategy. For instance, a previous study showed that sertraline, which is a selective inhibitor of central serotonin reuptake with well-established antidepressant and anxiolytic activity, exhibits a synergistic effect with fluconazole (FLC) against *Cryptococcus neoformans* in a *Galleria mellonella* model (Spitzer *et al*., 2011). More recently, clofazimine, a lipophilic riminophenazine antibiotic compound which has been in clinical use for almost 40 years, but almost nothing was known about its mechanism of action, acts synergistically with fluconazole against diverse fungal species (Robbins *et al*., 2015). In addition, the natural product beauvericin, also a cyclohexadepsipeptide mycotoxin, was found to effectively potentiate the activity of fluconazole against some major human fungal pathogens (Shekhar-Guturja *et al*., 2016b). These studies will boost the development of more systemic approaches to repurposing compounds for tackling the rising risk of fungal infection.

In this study, we provided strong evidence that ponatinib significantly potentiated fluconazole efficacy and exhibited a broad-spectrum antifungal effect against diverse fungal pathogens, including *C. albicans*, *S. cerevisiae* and *C. neoformans*. More importantly, synergy testing of ponatinib and fluconazole in resistant *C. albicans* strains resulted in a reversal of fluconazole resistance. Following the elucidation of the mechanism of action, we finally concluded that ponatinib potentiates the antifungal efficacy of fluconazole, providing clues for developing new therapeutic strategies against fungal infections.

Results

The combination of ponatinib with fluconazole exerts a broad-spectrum synergistic and fungicidal activity

Ponatinib, a multitargeted receptor tyrosine kinase (RTK) inhibitor, was identified through screening an FDA-approved drug library (L4200, TargetMol) (Mei *et al*., 2020). We observed that a combination of ponatinib (Pona) and fluconazole (FLC) exhibited a much stronger inhibitory effect on the growth of the wild type *C. albicans* strain SC5314, when compared with ponatinib or fluconazole alone (Fig. 1A–D, Fig. S1). To test whether the function of ponatinib is conserved, we examined its ability to potentiate the activity of fluconazole against a variety of other fungal pathogens. As expected, ponatinib significantly enhanced the antifungal activity of fluconazole against *S. cerevisiae* (Fig. 1E–H) and the major human fungal pathogen *C. neoformans* (Fig. 1I–L). The synergistic activity of ponatinib with fluconazole was further confirmed by the checkerboard assay ($FICI < 0.5$), showing a powerful antifungal combination with broad-spectrum activity against diverse human fungal pathogens (Odds, 2003; Jansen *et al*., 2009; Spitzer *et al*., 2011; Robbins *et al*., 2015; Shekhar-Guturja *et al*., 2016b) (Table 1). Moreover, we found through a lactate dehydrogenase (LDH) assay that a concentration of ponatinib at 16 μM or lower was considered non-toxic after incubation with the endothelial cells (Fig. S2).

Next, we performed time-kill curve analysis to determine if ponatinib renders fluconazole fungicidal. *Candida albicans* cells were subjected to fluconazole treatment with or without ponatinib in liquid medium, and the CFU ml^{-1} of the suspension from each treatment was counted after plating onto the YPD medium. With the increment of ponatinib concentration in the combination group, we observed that the number of survival colonies decreased gradually with time, revealing that ponatinib can transform fluconazole from fungistatic into fungicidal (Fig. 2A). The ability to switch between yeast and hyphal morphology is critical for *C. albicans* pathogenicity (Witchley *et al*., 2019). To examine whether the combinatorial antifungal effect could be attributed to an impact

Fig. 1. Combination of ponatinib and fluconazole synergistically inhibits growth of *C. albicans*, *S. cerevisiae* and *C. neoformans*. *C. albicans* (SC5314) (A–D), *S. cerevisiae* (BY4742) (E–H) and *C. neoformans* (H99) (I–L) isolates were subjected to twofold serial dilutions of fluconazole, ponatinib or both in YPD medium. OD_{600} was measured every 15 min at 30°C, and FICI was calculated using the reference guidelines for CLSI broth microdilution method (M38-A).

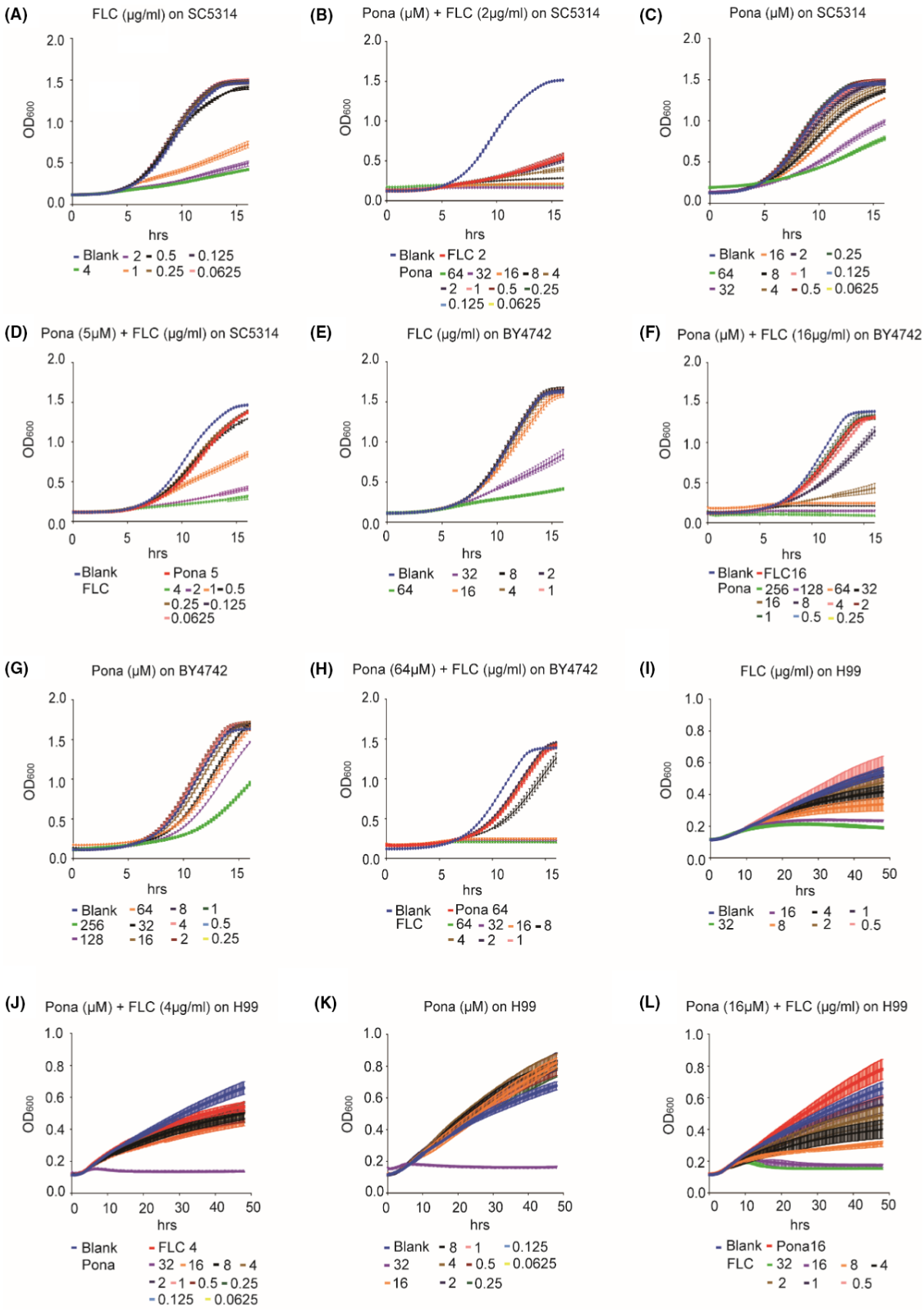

Table 1. Interaction between fluconazole and ponatinib against diverse human fungal pathogens by checkerboard microdilution assay.

	MIC alone		MIC combination			
Strain	FLC (μg ml^{-1})	Pona (μM)	FLC (μg ml^{-1})	Pona (μM)	FICI for combination	Mode of interaction
SC5314	0.5	16	0.0625	0.0625	0.13	Syn
BY4742	16	128	4	0.25	0.25	Syn
H99	4	32	0.5	0.125	0.13	Syn
CCC49	64	16	2	0.0625	0.04	Syn
CCC80	32	8	2	0.0625	0.07	Syn

Syn, Synergistic.

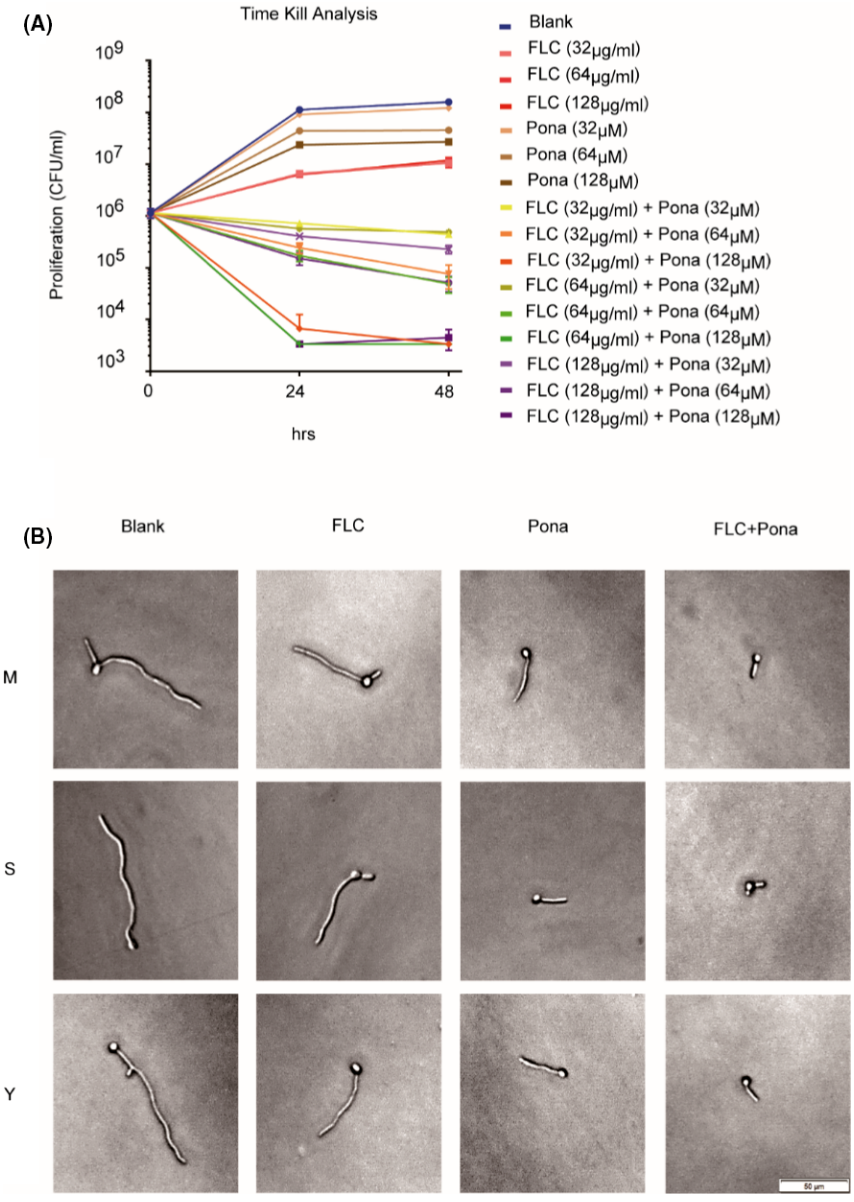

Fig. 2. Ponatinib transforms fluconazole from fungistatic into fungicidal and suppresses hyphal formation.
A. *C. albicans* (SC5314) cells were inoculated into YPD liquid medium supplemented with or without indicated compounds (DMSO, 32-128 μg/ml fluconazole, 32-128 μM ponatinib or both). The survival colony-forming units (CFUs) of SC5314 were counted after incubation at indicated periods of time (0, 24 and 48 h).
B. *C. albicans* (SC5314) cells were revived and resuspended in each of three different hyphae-inducing media (M199 buffered to pH8 with 50 mM MOPS; Spider; and YPD with 10% serum) containing DMSO, fluconazole (2 μg ml^{-1}), ponatinib (5 μM) or the combination. Cells were incubated at 37 °C, and hyphal morphology was checked under light microscope after 4 h of incubation.

on filamentation, we supplemented the hyphae-inducing media with fluconazole, ponatinib or both and evaluated the hyphal growth of *C. albicans*. The media we used in the assay include M199, Spider or YPD medium with 10% serum, which are all traditional hyphae-inducing media and have been widely used to assess the yeast–

hyphae morphological change in *C. albicans* (Toenjes *et al*., 2005; Liu *et al*., 2017; Lim *et al*., 2020; Yang *et al*., 2020). As shown in Fig. 2B, the inhibitory effect was much more significant in the combinatorial group. Thus, ponatinib potentiates fluconazole activity against diverse fungal pathogens and exerts a fungicidal activity with fluconazole.

Ponatinib prevents the emergence of azole resistance in C. albicans

Fluconazole resistance in the pathogenic yeast *C. albicans* poses significant challenges for the treatment and prevention of *Candida* infections frequently confronted by patients in clinic. We therefore investigated whether the combination of fluconazole and ponatinib can also be effective against the fluconazole-resistant clinical isolates of *C. albicans*. The minimal inhibitory concentration (MIC) values of fluconazole against two resistant isolates were 64 and 32 μg ml^{-1}, respectively, which were about 128- and 64-fold higher than that of the standard laboratory strain SC5314 (Fig. S3). Ponatinib combined with fluconazole was very efficient in the inhibition of the resistant strains, as we documented that ponatinib increased the susceptibility of resistant strains to fluconazole by up to eightfold and the effective concentration of fluconazole decreased from 64 to 8 μg ml^{-1} (Fig. 3B and F). In order to better evaluate the drug–drug interaction between ponatinib and fluconazole, we used the checkerboard assay as previously described (Rand *et al*., 1993) and calculated the FICI for the combination using a formula described in *Experimental procedures*. As shown in Table 1, ponatinib was highly synergistic with fluconazole with FICI = 0.04 for CCC49 and 0.07 for CCC80, highlighting its clinical applicability against fluconazole-resistant *C. albicans* isolates.

The above results prompted us to ask whether ponatinib could prevent the emergence of drug resistance, given that this event is often considered as a canonical case of evolution by natural selection (Shekhar-Guturja *et al*., 2016b; Vincent *et al*., 2016; Fransen *et al*., 2017). We plated 3×10^3 *C. albicans* cells onto YPD plates supplemented with 32 μg ml^{-1} fluconazole, 32 μM ponatinib or both. A plate without supplementation was used as a control. As shown in Fig. 3I, the emergence of resistance was significantly induced by fluconazole alone. However, the induction was potently suppressed by the combination of ponatinib. Our data further indicated that the desired final concentrations of fluconazole and ponatinib, which confer synergistic activity against drug-resistant *C. albicans* isolates, are 104.48 μM (32 μg ml^{-1}) and 32 μM respectively. Collectively, our results demonstrated that ponatinib not only enhances the antifungal activity against fluconazole-resistant isolates of *C. albicans* but also prevents the emergence of fluconazole resistance.

Ponatinib reduces efflux of fluconazole via Pdr5 and promotes the intracellular hyperaccumulation of fluconazole

Drug efflux is one of the most intensive investigated mechanisms for fluconazole resistance (Hampe *et al*., 2017). To test whether ponatinib might affect drug efflux to enhance the antifungal activity of fluconazole, we first screened the sensitivity of each of 16 *S. cerevisiae* mutants lacking individual ATP-binding cassette (ABC) transporter to ponatinib (Suzuki *et al*., 2011). The results showed that only the *pdr5Δ* mutant was hypersensitive to ponatinib treatment, indicating that ponatinib might interact with Pdr5 (Fig. 4A and B).

Pdr5 is an ABC transporter which pumps out a series of structurally unrelated compounds, including azoles and rhodamine (Prasad and Goffeau, 2012; Shekhar-Guturja *et al*., 2016b; de Moraes *et al*., 2020). Consistent with previous studies (Lamping *et al*., 2007; Prasad and Goffeau, 2012), we also confirmed that fluconazole is a substrate of Pdr5. First, we compared the vegetative growth of wild-type and *pdr5Δ* mutant cells in the absence and presence of fluconazole and the results showed that the mutant lacking *PDR5* exhibited hypersensitivity to fluconazole when compared to the wild type (WT). Next, we treated the WT with increasing concentrations of fluconazole and the cells were stained with Rhodamine 6G, which is a commonly used fluorescent dye for mimicking fluconazole efflux as both molecules share the same transporters in yeast (Maesaki *et al*., 1999). The assay measured the efflux activities in the yeast cells being incubated with fluconazole and ponatinib at increasing concentrations showing synergism based on the intensity of intracellular fluorescence (red colour). Beauvericin, known to effectively potentiate the activity of fluconazole against yeasts (Shekhar-Guturja *et al*., 2016a; Shekhar-Guturja *et al*., 2016b), was used as a control. Interestingly, the intracellular accumulation of Rhodamine 6G was found to correlate with the level of fluconazole (Fig. 4C, E). To assess the effect of ponatinib on Pdr5 activity, we examined rhodamine-6G efflux in wild-type *S. cerevisiae* strain BY4742 in incubation with beauvericin or fluconazole/ponatinib at the concentrations of ponatinib MIC showing synergism. We observed in Fig. 4D that the combinatorial use of fluconazole and ponatinib resulted in a dose-dependent accumulation of red fluorescence, suggestive of an effective inhibition of the efflux of rhodamine-6G. The results also supported a close association of the antifungal effects of the fluconazole/ponatinib combination with the function of efflux pumps in the yeast. Finally, qRT-

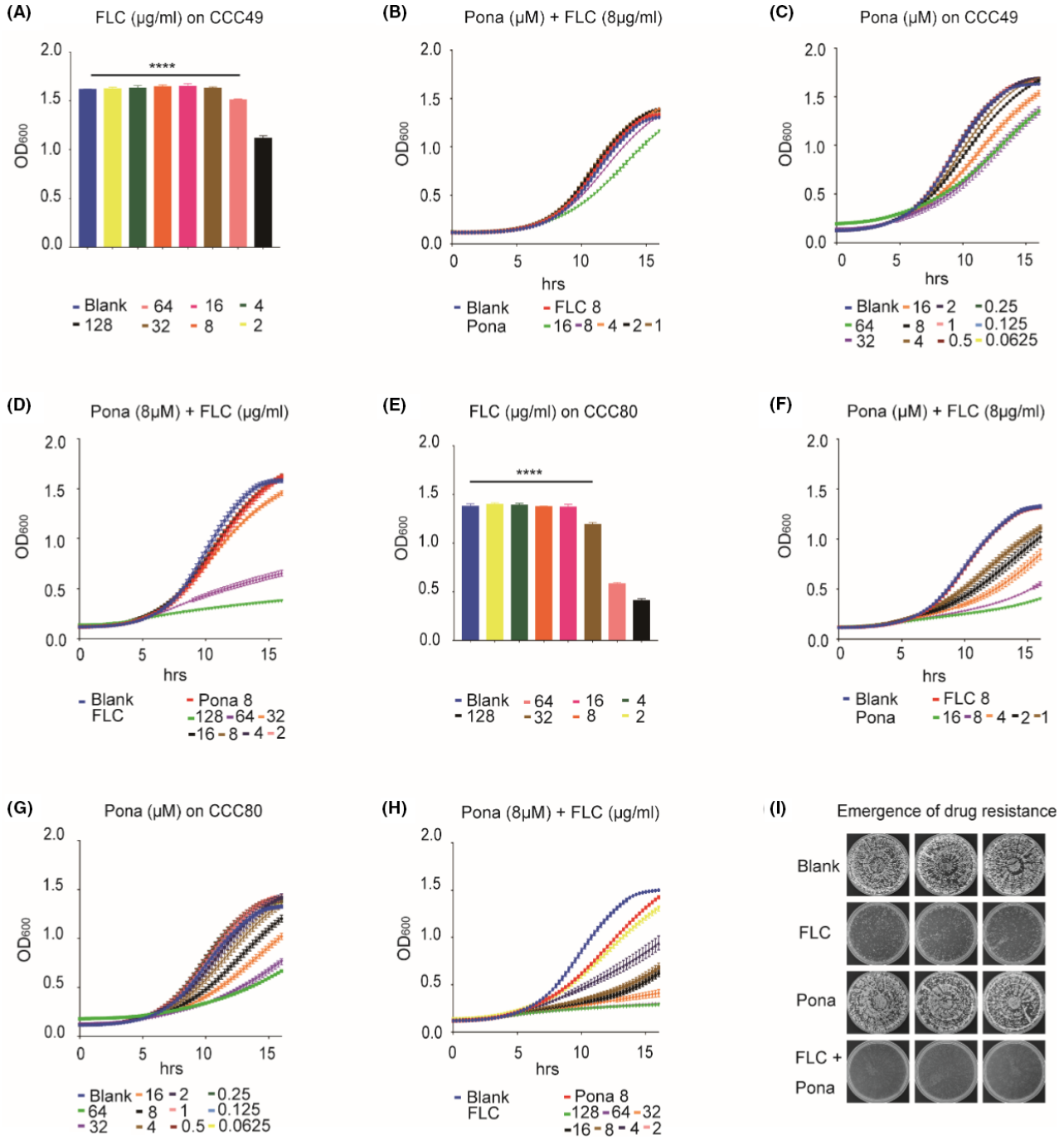

Fig. 3. Ponatinib acts synergistically with fluconazole against azole-resistant clinical isolates and prevents the emergence of resistance. CCC49 (A–D) and CCC80 (E–H) were subjected to twofold serial dilutions of fluconazole, ponatinib or both in YPD medium. OD_{600} was measured every 15 min at 30°C for 16 h, and FICI was calculated by standard CLSI broth microdilution method (M38-A).
I. *C. albicans* (SC5314) cells were inoculated into YPD plates containing indicated dosages of compounds (DMSO, 32 μg ml^{-1} fluconazole, 32 μM ponatinib, combination). The cell growth of resistant strains was observed after 3 days. ****$P < 0.0001$ vs. DMSO (the one-way ANOVA and Tukey multiple comparisons).

PCR analysis revealed that ponatinib treatment had no effect on the transcript levels of *PDR5* in *S. cerevisiae*, suggesting that ponatinib may only perturb the activity of Pdr5 instead of its transcription (Fig. S4). Taken together, our data clearly demonstrate that ponatinib improves the efficacy of fluconazole by stimulating intracellular fluconazole accumulation through inhibition of Pdr5.

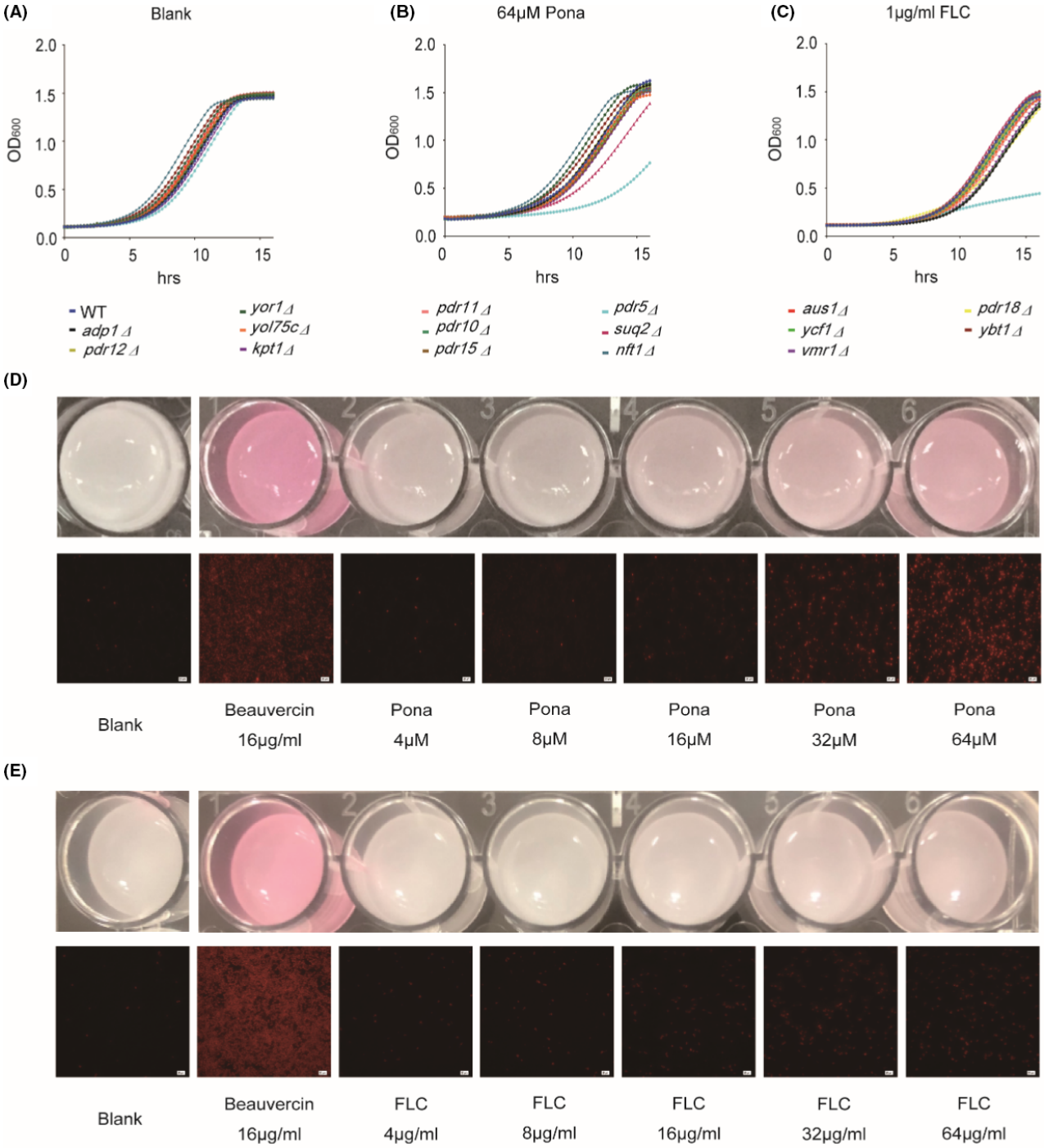

Fig. 4. Ponatinib enhances intracellular hyperaccumulation of fluconazole via Pdr5.
A–C. The *S. cerevisiae* WT and 16 ABC mutants were separately treated with Ponatinib or fluconazole at indicated concentrations.
D–E. BY4742 was pretreated with beauvericin, ponatinib or fluconazole, following by addition of the same concentration of rhodamine-6G. The intracellular accumulation of rhodamine-6G was observed under fluorescence microscopy.

Whole-genome sequencing identifies Pma1 as the putative target of ponatinib

Whole-genome sequencing is a technology widely exploited to identify the targets of antifungal agents in the model yeast *Saccharomyces cerevisiae* (Shekhar-Guturja *et al.*, 2016b). Our results in Fig. 1 showed that Ponatinib alone also harbours the inhibitory activity against the growth of yeast cells, implying the presence of additional targets. We therefore sought to identify the

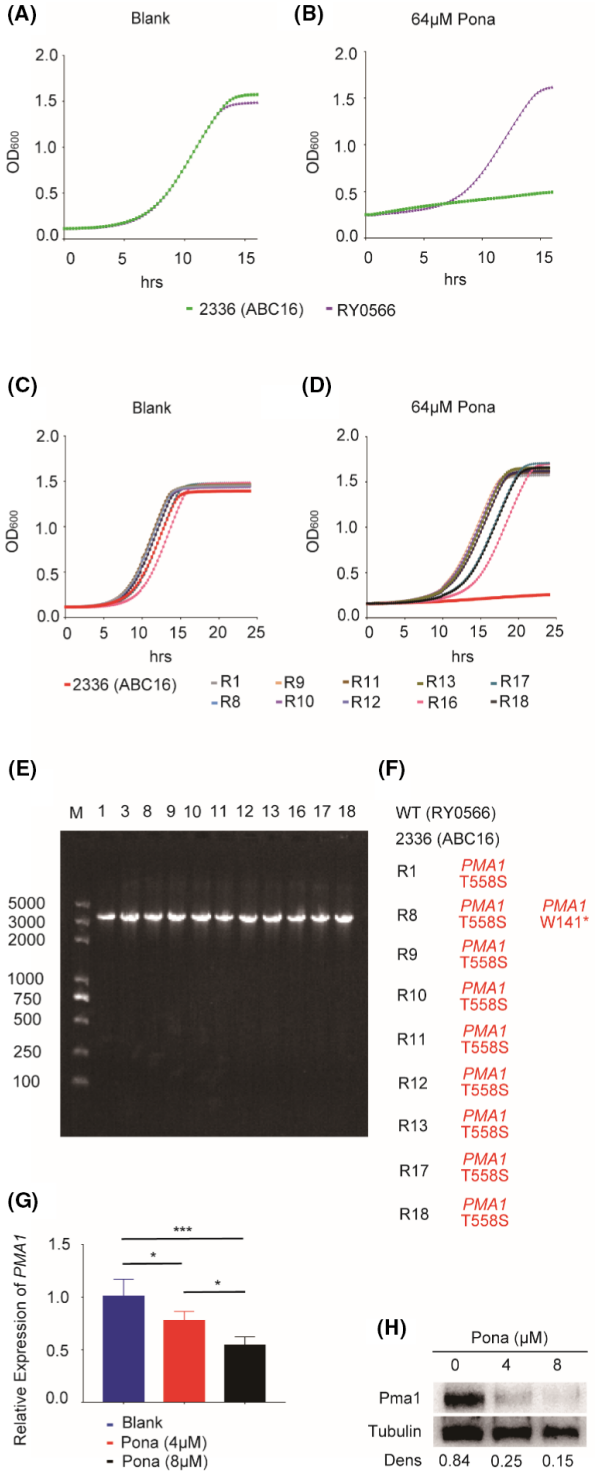

Fig. 5. Identification of the ponatinib target by whole-genome sequencing.
A–B. Strains RY0566 (wild type) and 2336 (the 16ABC mutant lacking all 16 efflux pump-encoding genes) were treated with ponatinib.
C–D. Strain 2336 and ponatinib-resistant mutants were treated with ponatinib.
E. Gel electrophoresis results of PCR products. DNA was extracted from drug-resistant mutant cells and was amplified by PCR. (F) Sequencing results of PCR products. Mutations identified by whole-genome sequencing of resistant mutants were indicated as amino acid changes. All resistant mutants harbour identical mutations in Pma1.
G. The total RNAs were extracted from the ABC16 mutant strain 2336 treated with ponatinib and prepared for qRT-PCR. Error bars represent SDs of three biological triplicates.
H. The protein extracts were prepared from the ABC16 mutant cells treated with ponatinib and subject to western analysis, using antibodies against Pma1 and tubulin respectively. Blots were quantified using Image J. Tubulin was used as a loading control. $*P < 0.05$; $***P < 0.001$ or $****P < 0.0001$ (the one-way ANOVA and Tukey multiple comparison).

target of ponatinib using the method of whole-genome sequencing. To do that, the predominant efflux effect of 16 ABC transporters, which are highly expressed in the yeast cells, has to be minimized or excluded firstly. We therefore conducted a screen for ponatinib-resistant isolates in the background of a specific *S. cerevisiae* mutant lacking all 16 ABC transporter-encoding genes (ABC16 strain; strain 2336) (Suzuki *et al*., 2011; Shekhar-Guturja *et al*., 2016b). The parental strain RY0566 was used as WT control. Specifically, about 3×10^7 cells ml^{-1} of ABC16 strain were plated onto YPD medium supplemented with 64 μM ponatinib and we randomly isolated and sequenced ten ponatinib-resistant colonies (Fig. 5A–D). Our whole-genome sequencing of the 10 isolates revealed that nine out of 10 mutants harboured the same missense mutation, T558S, in Pma1 (Fig. 5E and F). Interestingly, it has been reported that the P-type H^+-ATPase Pma1 is an essential proton pump able to regulate cytosolic pH homeostasis (Zhang *et al*., 2010), partly validating our screening results.

To further evaluate the relationship between ponatinib compound and Pma1 expression, we first quantified and compared the transcript levels of *PMA1* in the absence or presence of ponatinib. As shown in Fig. 5G, ponatinib significantly repressed the transcriptional expression of *PMA1* in a dose-dependent manner. Moreover, we found that Pma1 protein expression could also be modulated by ponatinib, as the immunoblot analysis clearly showed that the Pma1 protein levels were decreased dramatically by treating the cells with ponatinib, and the reduction is also dose-dependent (Fig. 5H). In microbial organisms, the extrusion of protons by the electron transport chain causes an electrochemical gradient of protons, known as the proton motive force (PMF), which is generated across the cell membrane (Mitchell, 2011). Given the role of ponatinib as an essential proton pump in regulation of cytosolic pH, we ask there may exist a possible relationship between PMF and the accumulation of intracellular fluconazole by ponatinib, in other words, the proton motive force (PMF) and drug efflux pumps may play a central role in the drug combination effect.

Our results showed that the enhancement of proton transport by increasing the proton motive force (PMF) after treatment with fluconazole, could be suppressed by supplementation of ponatinib (Fig. S5), further supporting the notion that ponatinib shows synergistic interaction when combined with fluconazole. Taken together, the results shown here highly support that Pma1 is the potential target of ponatinib (Fig. 6).

Discussion

The global incidence of fungal infection has increased over the last few decades due to the expanded ageing population, widespread azole resistance and the marked increase in the number of immunocompromised patients. Due to the fact that invasive fungal infections and fungal sepsis are rapidly increasing with considerable morbidity and mortality, especially in the intensive care unit (ICU), combinatorial antifungal therapy has been becoming a promising therapeutic strategy to enhance drug effectiveness and ameliorate the emergence of drug resistance and of course, has been gaining increasing attention within both industry and academia. Ponatinib is an FDA-approved oral tyrosine kinase inhibitor (Mitchell *et al.*, 2018) and has been evaluated to impede tumour progression, including tumours in thyroid, breast, ovary and lung, neuroblastoma, rhabdoid tumours, gastrointestinal stromal tumours, *et al* (Musumeci *et al.*, 2018). In this study, we discovered a novel function of this compound, which acts as a potentiator of azole activity against diverse human fungal pathogens, as well as the highly fluconazole-resistant isolates of *C. albicans*. Moreover, our work illustrated that the mechanism of the synergistic combinations that potentiate the antifungal fluconazole is associated with the inhibitory activity of ponatinib, as shown by inhibiting efflux of fluconazole via Pdr5 and suppressing the expression of the P-type H^+-ATPase Pma1. We provided evidence that ponatinib may execute two levels of actions in the synergism: First, it reduces efflux of fluconazole by inhibiting Pdr5 and thus promotes the intracellular hyperaccumulation of fluconazole; Second, it may interfere with the cytoplasmic pH homeostasis by affecting the expression of the putative target Pma1, as the P-type H^+-ATPase Pma1 has been reported to be an essential proton pump operating to regulate the cytosolic pH homeostasis (Zhang *et al.*, 2010). Importantly, the observation that the effective concentration of ponatinib appears to be non-toxic towards

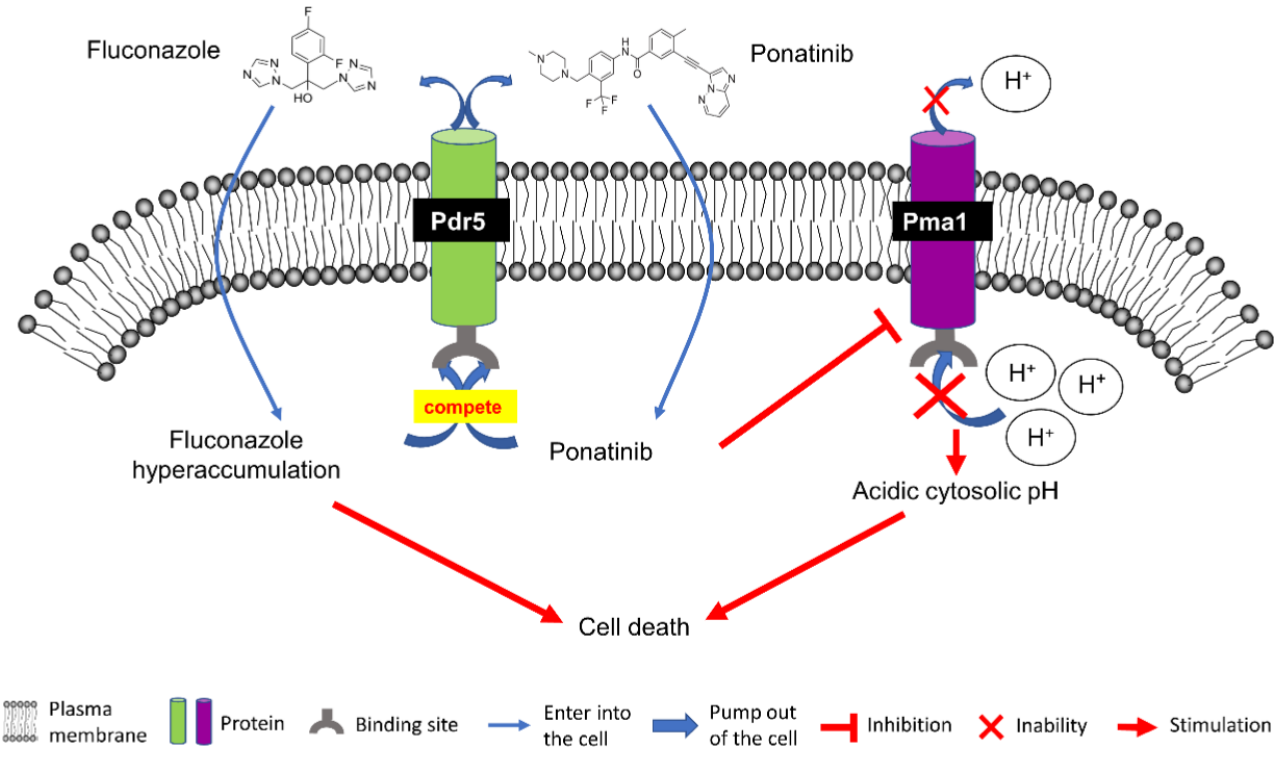

Fig. 6. Model depiction of the role of ponatinib in potentiation of the antifungal efficacy of fluconazole by inhibition of fluconazole efflux via Pdr5 and suppression of Pma1 expression. Ponatinib (PubChem CID: 24826799) promotes intracellular fluconazole (PubChem CID:3365) accumulation by binding to Pdr5. On the other hand, ponatinib perturbs the cytosolic pH homeostasis by inhibiting the proton pump Pma1 located at the plasma membrane. Eventually, the dual action of ponatinib through these two pathways leads to cell death.

endothelial cells greatly assists in dealing with the concern of the potential drug side-effect, which may limit its application in future translational studies. Of course, the interaction between ponatinib and fluconazole identified so far is certainly only the tip of the iceberg and awaits more systemic analysis.

Currently, the most urgent problem related to fungal infections in clinic is the emergence of multidrug resistance due to the fungistatic activity of antifungals like fluconazole. Identification of a novel antifungal candidate which can transform the fungistatic effect of fluconazole to fungicidal will be an effective strategy for clearance of fungal pathogens. Our results indicate that ponatinib not only inhibits the growth of a broad-spectrum of fungal pathogens but also converts fluconazole from fungistatic to fungicidal which prevents the emergence of azole resistance, providing a promising therapeutic strategy for antifungal development in the future.

The ABC (ATP-binding cassette) superfamily contains membrane proteins that transport a wide variety of substrates, such as metabolic products, lipids and sterols, and drugs, across extra- and intracellular membranes. In microbial organisms, the multidrug efflux pumps, which belong to members of the ABC superfamily, act to effectively pump drugs out of cells, significantly reduce the intracellular concentration of antifungals and prevent the emergence of drug resistance (Nakamura *et al*., 2001; Coste *et al*., 2006; Shapiro *et al*., 2011). Among them, Pdr5 is the most abundant ABC transporter in *S. cerevisiae* and shares sequence homology with Cdr1 in *C. albicans* (Kontoyiannis and Lewis, 2002). Studies have revealed that Pdr5 is able to squeeze out hundreds of structurally independent hydrophobic compounds to pass through the plasma membrane (Kolaczkowski *et al*., 1996; Egner *et al*., 1998; Golin *et al*., 2003). Intriguingly, Pdr5 was the only target that came out of the screen when we used the 16 ABC transporter mutants to evaluate the efflux effect of ponatinib, suggesting that Pdr5 could be the substrate of Ponatinib and by inactivating the activity of Pdr5, the compound prevents the efflux of fluconazole from the fungal cells. In the future, more evidence is required to support our hypothesis, especially those implicated in assaying direct interaction between Pdr5 and ponatinib.

The cytosolic pH homeostasis plays a key role in cell growth (Gillies *et al*., 1981, Casey *et al*., 2010, Dechant *et al*., 2010, Dechant *et al*., 2014, Martínez-Muñoz and Kane, 2017; Saliba et al., 2018). The ability to regulate intracellular pH enables *C. albicans* to survive in both extremely acidic and alkaline microenvironments (Casey *et al*., 2010; Cyert and Philpott, 2013; Felcmanova et al., 2017; Martínez-Muñoz and Kane, 2017; Saliba et al., 2018; Xu *et al*., 2019). The critical elements determining pH homeostasis are as follows: proton pumps, exchangers and buffers (Casey *et al*., 2010). Proton pumps, such as Pma1 in the plasma membrane, are required to establish certain pH gradient (Ferreira *et al*., 2001; Orij *et al*., 2011; Martínez-Muñoz and Kane, 2017). Exchangers can transport ions and solutes against the gradient by using the energy stored in pH gradients or ion gradients to determine the final pH (Brett *et al*., 2005; Ohgaki et al., 2011; Kondapalli *et al*., 2014). Buffers protect the cells or organelles from the disturbance of short-term pH fluctuation (Casey *et al*., 2010; Poznanski *et al*., 2013). Pma1, which is independent of ion pumps, is a structural component of the plasma membrane accounting for 20–40% of the total plasma membrane proteins (Monk *et al*., 1991). Strikingly, this P-type H^+-ATPase plays a key role in cytosolic pH regulation (Serrano, 1988; van der Rest *et al*., 1995) by pumping the proton out of the cells and consuming an impressive amount of intracellular ATP which accounts for approximately a quarter of total ATP consumption (Giacomello *et al*., 2013), highlighting the potential of Pma1 as an antifungal target. Interestingly, harnessing whole-genome sequencing and RT-PCR analysis, we argued that ponatinib may target Pma1 to perturb the pH homeostasis in the cytoplasm, eventually leading to cell death. Supporting this proposition requires more evidence; however, the effective inhibitor of Pma1 has not been determined in clinic (Stewart *et al*., 1988; Monk *et al*., 1995; Perlin *et al*., 1997; Monk *et al*., 2005; Chan *et al*., 2007; Billack *et al*., 2009; Ottilie *et al*., 2018). Thus, alternative strategies have to be considered.

Numerous studies have demonstrated that fluconazole is widely used in clinic for the treatment of fungal infection by selectively interfering with the activity of cytochrome P-450 and inhibiting the biosynthesis of ergosterol in the plasma membrane. However, targeting a single drug target is usually difficult to achieve the desired effect and prone to drug resistance. In our work, we found that ponatinib acts as a fluconazole potentiator through suppression of not only multidrug efflux via Pdr5 but also Pma1 expression in vitro, supporting that the multi-target drug ponatinib could enhance the effectiveness of fluconazole via two action modes. Compared with the single drug administration, drug combinatorial therapy has demonstrated great advantages in overcoming drug resistance and improving therapeutic efficacy, since this therapy harbours multi-target activities and confers high information-processing capacity and functional diversity, especially the simultaneous regulation of multiple inputs into the signalling network. Moreover, the drug combinatorial therapy allows many parts of the network to be activated at once and has been applied in the treatment of many chronic diseases such as cancer and thus has drawn intensive attention from researchers and pharmaceutical enterprises. Of course, it has to be

noted that the main problem faced by repurposing the existing multi-target drugs is their potential adverse effects. In addition, the optimal drug concentration for each target is often different, and it is difficult for a multi-target drug to achieve the optimal pharmacological effect for each target, which may affect its synergistic effect. Thus, testing clinically relevant pharmacodynamics and pharmacokinetics of the prioritized drug combinations needs to be seriously considered for identification, development and optimization of efficacious combinatorial drug treatments.

Experimental procedures

Strains and culture condition

The strains used in this study (Table 2) were stored at −80°C and routinely grown in yeast peptone dextrose (YPD) medium.

Minimal Inhibitory Concentration (MIC) Assay

MIC assay was evaluated in 96-well microtitre plates using the broth dilution testing reference method M27-A3/S4, as recommended by the Clinical and Laboratory Standards Institute (CLSI) (Rex, 2008). Twofold serial dilutions of fluconazole (HY-B0101; MedChemExpress, Shanghai, China) or ponatinib (S1490; Selleck, Shanghai, China) were prepared along the columns or rows of a 96-well plate. Overnight cultures were diluted to an OD_{600} of 1.0, followed by another 100-fold dilution to reach a final OD_{600} of ~ 0.01 (Chen *et al.*, 2011; Chen and Noble, 2012). The plates were incubated at 30°C and photographed by ChemiDoc MP (Bio-Rad, Shanghai, China). The MIC was defined as the lowest drug concentration that caused a specified reduction in visible growth comparing with that of control. All strains were assessed in biological triplicates with three technical replicates.

LDH Assay

To test the cytotoxicity of ponatinib on mammalian cells, 2×10^4 endothelial cells (NCM460) were seeded overnight in Dulbecco's modified Eagle's medium (DMEM) supplemented with 10% FBS and kept at 37°C in a CO_2 incubator. Cells were then exposed to twofold serial dilutions of ponatinib for 1.5 h at 37°C before being lysed. Cytotoxicity was measured using Cytotoxicity LDH Assay Kit-WST (NG715, DOJINDO, Shanghai, China).

Checkerboard assay

Checkerboard assay was evaluated in 96-well microtitre plates using the reference guidelines for broth microdilution method (M38-A2) from the Clinical and Laboratory Standards Institute (CLSI) (Alexander, 2008). The procedures were performed as described in a previous study (Hsieh *et al.*, 1993). Briefly, each compound was serially diluted in two-fold in a 96-well plate, either across columns of the plates (fluconazole) or rows of the plates (ponatinib). Overnight cultures were diluted to an OD_{600} of 1.0, followed by another 100-fold dilution to reach a final OD_{600} of ~ 0.01 (Chen *et al.*, 2011; Chen and Noble, 2012). The plates were incubated at 30°C, and the OD_{600} was measured every 15min. The fractional inhibitory concentration index (FICI) of each drug combination was determined according to the standard CLSI protocol, and FICI < 0.5 was defined as synergy (Brown *et al.*, 2014). The formula is calculated as follows: $FICI = (MIC_{A\ in\ combination}/MIC_{A\ alone}) + (MIC_{B\ in\ combination}/MIC_{B\ alone})$.

Filamentation assay

Optimal induction of filamentous growth in *C. albicans* was achieved by incubating the yeast cells on hyphal-inducing medium, following the procedures described previously (Flanagan et al., 2017).

Emergence of drug resistance in vitro

For emergence of drug resistance in vitro, fresh overnight yeast cultures were washed twice in PBS and diluted into an optical density (OD_{600}) of 0.5. After 10-fold serial dilutions, cells were spread onto appropriate agar plates supplemented with 32 μg ml^{-1} fluconazole, 32 μM ponatinib or both.

Time-kill curve analysis

Overnight culture of *C. albicans* was diluted to a final OD_{600} of 0.05 in liquid YPD medium containing fluconazole (32, 64, 128 μg ml^{-1}), ponatinib (32, 64, 128 μM) or both in 96-well plates with a final volume of 200 μl. The suspension was diluted at 1:250 000 and plated on YPD plates at indicated periods of time (0, 24 h or 48 h). The plates were incubated at 30°C for 24 h before determining the colony-forming units (CFUs) by counting.

Rhodamine-6G (R6G) staining assay

Cells grown overnight in YPD liquid medium at 30 °C were washed with ice-cold glucose-free phosphate-buffered saline (PBS) and incubated at 30°C for 1 h under starvation to reduce the ATP-binding cassette (ABC) efflux pumps activity. The collected cells were then washed and diluted to 10^8 cells ml^{-1} in ice-cold PBS, which were exposed to 4, 8, 16, 32, 64 μM ponatinib or

Table 2. Strains used in this study.

Strain name	Parent	Genotype	Strain background /construction	References
C. albicans				
SC5314		Wild type		This work
CCC49			Fluconazole-resistant clinical isolates	This work
CCC80			Fluconazole-resistant clinical isolates	This work
S. cerevisiae				
BY4742		Wild type		Suzuki *et al.* (2011)
adp1Δ	BY4742		*adp1Δ* transformed with WT	Suzuki *et al.* (2011)
snq2Δ	BY4742		*snq2Δ* transformed with WT	Suzuki *et al.* (2011)
ycf1Δ	BY4742		*ycf1Δ* transformed with WT	Suzuki *et al.* (2011)
pdr15Δ	BY4742		*pdr15Δ* transformed with WT	Suzuki *et al.* (2011)
yor1Δ	BY4742		*yor1Δ* transformed with WT	Suzuki *et al.* (2011)
vmr1Δ	BY4742		*vmr1Δ* transformed with WT	Suzuki *et al.* (2011)
pdr11Δ	BY4742		*pdr11Δ* transformed with WT	Suzuki *et al.* (2011)
nft1Δ	BY4742		*nft1Δ* transformed with WT	Suzuki *et al.* (2011)
kpt1Δ	BY4742		*kpt1Δ* transformed with WT	Suzuki *et al.* (2011)
ybt1Δ	BY4742		*ybt1Δ* transformed with WT	Suzuki *et al.* (2011)
pdr18Δ	BY4742		*pdr18Δ* transformed with WT	Suzuki *et al.* (2011)
yol075cΔ	BY4742		*yol075cΔ* transformed with WT	Suzuki *et al.* (2011)
aus1Δ	BY4742		*aus1Δ* transformed with WT	Suzuki *et al.* (2011)
pdr5Δ	BY4742		*pdr5Δ* transformed with WT	Suzuki *et al.* (2011)
pdr10Δ	BY4742		*pdr10Δ* transformed with WT	Suzuki *et al.* (2011)
pdr12Δ	BY4742		*pdr12Δ* transformed with WT	Suzuki *et al.* (2011)
BY4741		Wild type		
RY0566	BY4741	Isogenic control MATa *hΔ::tetO2-GFP-URA3 can1Δ::GMToolkit -a [CMVpr-rtTA KANMX4 STE2pr-Sp-his5]lyp1Δ his3Δ1 leu2Δ0 ura3Δ0 met15Δ0*		Suzuki *et al.* (2011)
2336	BY4741	Green Monster MATa *adp1Δ snq2Δ ycf1Δ pdr15Δ yor1Δ vmr1Δ pdr11Δ nft1Δ bpt1Δ ybt1Δ ynr070wΔ yol075Δ aus1Δ pdr5Δ pdr10Δ pdr12Δ can1Δ:: GMT oolkit-a (CMVpr-rtTA KANMX4 STE2pr-Sp-his5) his3Δ1 leu2Δ0 ura3Δ0 met15Δ0* Each ABC-transporter deletion contains ADHterm-tetO2pr-GFP(S65T)-CYC1termURA3.		Suzuki *et al.* (2011)
R1	2336		Ponatinib resistant isolate	This work
R8	2336		Ponatinib resistant isolate	This work
R9	2336		Ponatinib resistant isolate	This work
R10	2336		Ponatinib resistant isolate	This work
R11	2336		Ponatinib resistant isolate	This work
R12	2336		Ponatinib resistant isolate	This work
R13	2336		Ponatinib resistant isolate	This work
R16	2336		Ponatinib resistant isolate	This work
R17	2336		Ponatinib resistant isolate	This work
R18	2336		Ponatinib resistant isolate	This work
C. neoformans				
H99		Wild type		This work

4, 8, 16, 32, 64 μg ml^{-1} fluconazole respectively. Beauvericin at a concentration of 16 μg ml^{-1} was added as a positive control with dimethyl sulfoxide (DMSO) as the negative control. All samples were incubated for another 2 h at 30°C. After treatment with 10 μM (final concentration) R6G, cells were incubated for another 1.5 h at 30°C. The external R6G was then removed by washing with PBS, and 2% glucose was added to the samples to reactivate the ABC efflux pumps. After incubation at 30°C for 1 h, the reactivated cells were washed and observed under fluorescent microscopy to monitor intracellular R6G accumulation.

Whole-genome sequencing of ponatinib-resistant isolates

The parental strain ABC16 and 10 selected ponatinib-resistant isolates were separately cultured on solid YPD plates for DNA extraction. Then, the mutations in *PMA1* of the above 11 isolates were validated by PCR and sequencing to identify the specific mutation (Heitman *et al*., 1991; Shekhar-Guturja *et al*., 2016b; Vincent *et al*., 2016; Sukheja et al., 2017; Wang *et al*., 2020). The PCR reaction mixture is comprised of 10xHifi PCR buffer (2 μl), 2 mM dNTPs (1.2 μl), 50 mM $MgSO_4$ (0.6 μl), 10 mM primers (0.4 μl), 5 μM Taq Enzyme (0.1 μl), DNA template (2 μl) and sterile water up to μl. For the PCR program, the conditions are followed by 95°C 5 min; 94°C 30 s, 55°C 30 s and 68°C 6 min and 40 s for 30 cycles; 68°C 10 min. The genomic sequences of all strains can be accessed through NCBI accession number PRJNA649097.

qRT-PCR

Overnight cell cultures in YPD at 30°C were diluted to OD_{600} of 1.0. Cells were treated with DMSO, fluconazole, ponatinib or both and grown at 30°C for 3 h. The RNA was then extracted by hot phenol method and further treated with RT reagent with gDNA Eraser (Takara #RR047A, Beijing, China). The PCR was performed using Universal SYBR Green Supermix (Bio-Rad #1725121) with the following program: 95°C for 30 s; 95°C for 5 s; and 60°C for 30 s, for 40 cycles. Primers are listed in Table 3. The data were analysed by the $2^{-\Delta\Delta Ct}$ method, in which $\Delta\Delta C_t$ = (C_t value of target gene − C_t value of reference gene)$_{sample}$ − (C_t value of target gene − C_t value of reference gene)$_{control}$, as described previously (Livak and Schmittgen, 2001; Huang *et al*., 2007).

Western blot

The cell lysis, protein extraction and Western blot procedures were performed as described in a previous study (Liu *et al*., 2017). The antibodies are listed in Table 4. For densitometry, Image J software (https://imagej.net/Downloads) was used as in a previous study (Flanagan et al., 2017).

Proton pump in plasma membrane

The BY4741 strain was cultured overnight in YPD liquid medium at 30°C, and 5×10^8 cells were used for extraction of IOV (In-side out), which was treated with fluconazole (16 μg ml^{-1}), ponatinib (8 μM) or both in 96 well black plates. The fluorescence intensity at excitation wavelength 490 nm and emission wavelength 530 nm was measured every 5 min for 1 h. The *N*-ethylmaleimide (NEM) (10 μM) and orthovanadate (OV) (100 μM) were added as a positive control with dimethyl sulfoxide (DMSO) as the negative control (Van Dyke *et al*., 1985, Kaunitz and Sachs, 1986). IOV (In-side out) was extracted using Fungus/Yeast Membrane Vesicle RSOV/IOV Prep Kit (GMS 10169.3 v.A; Shanghai CHENGONG Biotechnology Co., Ltd, Shanghai, China). The proton pump in the plasma membrane was mea-

Table 3. Primers used in this study.

Primer name	Purpose	Sequence 5' to 3'
NL50	Forward to amplify *PMA1*	ACATTCAAAAGAAAGAAAAAAAATATACCCCAGCTAGTT-AAAGAAAATCATTGAAAAGAATAAGAAGATAAGAAAGA-TTTAATTATCAAACAATATCAATCGGATCCCCGGGTTAATTAA
NL51	Reverse to amplify *PMA1*	TTGATAAAAAAATTAAAATTAAAATTAGAAAAATTAAACCAGAAA-AATCAAGTTGATTAAAATGTGACAAAAATTATGATTAAATGC-TACTTCAACAGGAGAATTCGAGCTCGTTTAAAC
NL220	Forward for qRT-PCR of *PMA1*	GCCTGCTAAGACTTACGATGACGC
NL221	Reverse for qRT-PCR of *PMA1*	TTCACCGGCGGCAACTGGAC
NL222	Forward for qRT-PCR of *ACT1*	ATTATATGTTTAGAGGTTGCTGCTTTGG
NL223	Reverse for qRT-PCR of *ACT1*	CAATTCGTTGTAGAAGGTATGATGCC

Table 4. Antibodies used in this study.

Antibodies purpose	Antigen recognized	Species	Source or reference
Loading control	Tubulin	Rat	Abcam, #ab6161, Shanghai, China
	Pma1	Mouse	Gene Tex, #GTX24645, Alton Pkwy Irvine, CA, USA
Secondary	Rat Ig	Goat	Cell Signaling TECHNOLOGY, #7077, Shanghai, China
Secondary	Mouse Ig	Goat	Arigo, #65350, Shanghai, China

sured using Proton Transport (P ATPase dependent) Assay Kit (GMS 10159.1.2 v.A; Shanghai CHENGONG Biotechnology Co., Ltd).

Statistics

All data were shown as the mean ± SDs in three independent experiments. All results were calculated from the means of three separate experiments. Statistical analysis was performed using GraphPad Prism 7, San Diego, CA, USA with the one-way ANOVA and Tukey multiple comparison analysis at a $*P < 0.05$、$***P < 0.001$ or $****P < 0.0001$ level of significance.

Acknowledgements

This study was supported by grants from the National Key R&D Program of China (2018YFC2000700; 2020YFA0907200), the National Nature Science Foundation (81630086, 81971993, 31900129, 81572053, 31870141, 31570140), the Key Research Program (ZDRW-ZS-2017-1; KGFZD-135-19-11; 153831KYSB2-0170043) of the Chinese Academy of Sciences, the Major Science and Technology Innovation Program of Shanghai Municipal Education Commission (2019-01-07-00-01-E00059), the Program for Young Eastern Scholar at Shanghai Institutions of Higher Learning (program QD2018016), Shanghai Pujiang Program (18PJ1406600), Innovative research team of high-level local universities in Shanghai, the Innovation Capacity Building Project of Jiangsu Province (BM2020019).

The authors thank Prof. Julia R. Koehler, Prof. Jinqiu Zhou and Prof. Ling Lu for kindly providing strains used in this work and all the lab members in Shanghai Jiao Tong University School of Medicine and at Institut Pasteur of Shanghai, Chinese Academy of Sciences, for their help in discussion and preparation of the manuscript.

Funding Information

This study was supported by grants from the National Key R&D Program of China (2018YFC2000700; 2020YFA0907200), the National Nature Science Foundation (81630086, 81971993, 31900129, 81572053, 31870141, 31570140), the Key Research Program (ZDRW-ZS-2017-1; KGFZD-135-19-11;153831KYSB2-0170043) of the Chinese Academy of Sciences, the Major Science and Technology Innovation Program of Shanghai Municipal Education Commission (2019-01-07-00-01-E00059), the Program for Young Eastern Scholar at Shanghai Institutions of Higher Learning (program QD2018016), Shanghai Pujiang Program (18PJ1406600), Innovative research team of high-level local universities in Shanghai, the Innovation Capacity Building Project of Jiangsu Province (BM2020019).

Conflict of interests

The authors declare no conflicts of interest.

Author contribution

NNL, HW and CC conceived and designed the study; LL, NNL, HW and CC performed data analysis and wrote the manuscript; LL, TJ, YM, JZ, JL, JT, LW, JL and PY conducted all experiments and performed the statistical analysis of the data; LL, YP, HW, LZ, J.L.L.-R., RSS, CC, NNL and HW discussed the experiments and results.

Data Availability Statement

The data sets generated from the current study have been deposited in the US National Center for Biotechnology Information (NCBI). The accession number for the gene expression profiling raw data reported in this paper is NCBI PRJNA: 649097. The Submission ID is SUB7844246. The link is provided in https://submit.ncbi.nlm.nih.gov/subs/bioproject/SUB7844246/overview.

References

Alexander, B.D. (2008) *Reference Method for Broth Dilution Antifungal Susceptibility Testing of Yeasts*. Approved Standard M38-A2, Clinical and Laboratory Standards Institute.

Anderson, T.M., Clay, M.C., Cioffi, A.G., Diaz, K.A., Hisao, G.S., Tuttle, M.D., *et al*. (2014) Amphotericin forms an extramembranous and fungicidal sterol sponge. *Nat Chem Biol* **10:** 400–406.

Basso, V., Tran, D.Q., Ouellette, A.J., and Selsted, M.E. (2020) Host defense peptides as templates for antifungal drug development. *J Fungi* **6:** 241.

Billack, B., Santoro, M., and Lau-Cam, C. (2009) Growth inhibitory action of ebselen on fluconazole-resistant *Candida albicans*: role of the plasma membrane H+-ATPase, Microbial drug resistance. *(Larchmont N.Y.)* **15:** 77–83.

Brett, C.L., Tukaye, D.N., Mukherjee, S., and Rao, R. (2005) The yeast endosomal Na+K+/H+ exchanger Nhx1 regulates cellular pH to control vesicle trafficking. *Mol Biol Cell* **16:** 1396–1405.

Brown, J.C.S., Nelson, J., VanderSluis, B., Deshpande, R., Butts, A., Kagan, S., *et al*. (2014) Unraveling the biology of a fungal meningitis pathogen using chemical genetics. *Cell* **159:** 1168–1187.

Casey, J.R., Grinstein, S., and Orlowski, J. (2010) Sensors and regulators of intracellular pH. *Nat Rev: Mol Cell Biol* **11:** 50–61.

Chan, G., Hardej, D., Santoro, M., Lau-Cam, C., and Billack, B. (2007) Evaluation of the antimicrobial activity of

ebselen: role of the yeast plasma membrane H+-ATPase. *J Biochem Mol Toxicol* **21:** 252–264.

Chen, C., and Noble, S.M. (2012) Post-transcriptional regulation of the Sef1 transcription factor controls the virulence of *Candida albicans* in its mammalian host. *PLoS Pathog* **8:** e1002956.

Chen, C., Pande, K., French, S.D., Tuch, B.B., and Noble, S.M. (2011) An iron homeostasis regulatory circuit with reciprocal roles in *Candida albicans* commensalism and pathogenesis. *Cell Host Microbe* **10:** 118–135.

Coste, A., Turner, V., Ischer, F., Morschhäuser, J., Forche, A., Selmecki, A., *et al*. (2006) A mutation in Tac1p, a transcription factor regulating CDR1 and CDR2, is coupled with loss of heterozygosity at chromosome 5 to mediate antifungal resistance in *Candida albicans*. *Genetics* **172:** 2139–2156.

Cyert, M.S., and Philpott, C.C. (2013) Regulation of cation balance in *Saccharomyces cerevisiae*. *Genetics* **193:** 677–713.

de Moraes, D.C., Cardoso, K.M., Domingos, L.T.S., do Carmo Freire Ribeiro Pinto, M., Monteiro, R.Q., and Ferreira-Pereira, A. (2020) β-Lapachone enhances the antifungal activity of fluconazole against a Pdr5p-mediated resistant *Saccharomyces cerevisiae* strain. *Braz J Microbiol* **51:** 1051–1060.

Dechant, R., Binda, M., Lee, S.S., Pelet, S., Winderickx, J., and Peter, M. (2010) Cytosolic pH is a second messenger for glucose and regulates the PKA pathway through V-ATPase. *EMBO J* **29:** 2515–2526.

Dechant, R., Saad, S., Ibáñez, A.J., and Peter, M. (2014) Cytosolic pH regulates cell growth through distinct GTPases, Arf1 and Gtr1, to promote Ras/PKA and TORC1 activity. *Mol Cell* **55:** 409–421.

Egner, R., Rosenthal, F.E., Kralli, A., Sanglard, D., and Kuchler, K. (1998) Genetic separation of FK506 susceptibility and drug transport in the yeast Pdr5 ATP-binding cassette multidrug resistance transporter. *Mol Biol Cell* **9:** 523–543.

Felcmanova, K., Neveceralova, P., Sychrova, H., and Zimmermannova, O. (2017) Yeast Kch1 and Kch2 membrane proteins play a pleiotropic role in membrane potential establishment and monovalent cation homeostasis regulation. *FEMS Yeast Research* **17:** https://doi.org/10.1093/femsyr/fox053

Ferreira, T., Mason, A.B., and Slayman, C.W. (2001) The yeast Pma1 proton pump: a model for understanding the biogenesis of plasma membrane proteins. *J Biol Chem* **276:** 29613–29616.

Flanagan, P.R., Liu, N.-N., Fitzpatrick, D.J., Hokamp, K., Köhler, J.R., and Moran, G.P. (2017) The *Candida albicans* TOR-activating GTPases Gtr1 and Rhb1 Coregulate starvation responses and biofilm formation. *mSphere* **2:** e00477–17. https://doi.org/10.1128/mSphere.00477-17

Fransen, F., Hermans, K., Melchers, M.J.B., Lagarde, C.C.M., Meletiadis, J., and Mouton, J.W. (2017) Pharmacodynamics of fosfomycin against ESBL- and/or carbapenemase-producing Enterobacteriaceae. *J Antimicrob Chemother* **72:** 3374–3381.

Giacomello, M., De Mario, A., Scarlatti, C., Primerano, S., and Carafoli, E. (2013) Plasma membrane calcium ATPases and related disorders. *Int J Biochem Cell Biol* **45:** 753–762.

Gillies, R.J., Ugurbil, K., den Hollander, J.A., and Shulman, R.G. (1981) 31P NMR studies of intracellular pH and phosphate metabolism during cell division cycle of *Saccharomyces cerevisiae*. *Proc Natl Acad Sci USA* **78:** 2125–2129.

Golin, J., Ambudkar, S.V., Gottesman, M.M., Habib, A.D., Sczepanski, J., Ziccardi, W., and May, L. (2003) Studies with novel Pdr5p substrates demonstrate a strong size dependence for xenobiotic efflux. *J Biol Chem* **278:** 5963–5969.

Gray, K.C., Palacios, D.S., Dailey, I., Endo, M.M., Uno, B.E., Wilcock, B.C., and Burke, M.D. (2012) Amphotericin primarily kills yeast by simply binding ergosterol. *Proc Natl Acad Sci USA* **109:** 2234–2239.

Hampe, I.A.I., Friedman, J., Edgerton, M., and Morschhäuser, J. (2017) An acquired mechanism of antifungal drug resistance simultaneously enables *Candida albicans* to escape from intrinsic host defenses. *PLoS Pathog* **13:** e1006655.

Heitman, J., Movva, N.R., and Hall, M.N. (1991) Targets for cell cycle arrest by the immunosuppressant rapamycin in yeast. *Science (New York N.Y.)* **253:** 905–909.

Hsieh, M.H., Yu, C.M., Yu, V.L., and Chow, J.W. (1993) Synergy assessed by checkerboard a critical analysis. *Diag Microbiol Infect Dis* **16:** 343–349.

Huang, C., Yang, L., Li, Z., Yang, J., Zhao, J., Dehui, X.u., *et al*. (2007) Detection of CCND1 amplification using laser capture microdissection coupled with real-time polymerase chain reaction in human esophageal squamous cell carcinoma. *Cancer Genet Cytogenet* **175:** 19–25.

Jansen, G., Lee, A.Y., Epp, E., Fredette, A., Surprenant, J., Harcus, D., *et al*. (2009) Chemogenomic profiling predicts antifungal synergies. *Mol Syst Biol* **5:** 338.

Kaunitz, J.D., and Sachs, G. (1986) Identification of a vanadate-sensitive potassium-dependent proton pump from rabbit colon. *J Biol Chem* **261:** 14005–14010.

Kolaczkowski, M., van der Rest, M., Cybularz-Kolaczkowska, A., Soumillion, J.P., Konings, W.N., and Goffeau, A. (1996) Anticancer drugs, ionophoric peptides, and steroids as substrates of the yeast multidrug transporter Pdr5p. *J Biol Chem* **271:** 31543–31548.

Kondapalli, K.C., Prasad, H., and Rao, R. (2014) An inside job: how endosomal Na(+)/H(+) exchangers link to autism and neurological disease. *Front Cell Neurosci* **8:** 172.

Kontoyiannis, D.P., and Lewis, R.E. (2002) Antifungal drug resistance of pathogenic fungi. *Lancet (London, England)* **359:** 1135–1144.

Lamping, E., Monk, B.C., Niimi, K., Holmes, A.R., Tsao, S., Tanabe, K., *et al*. (2007) Characterization of three classes of membrane proteins involved in fungal azole resistance by functional hyperexpression in *Saccharomyces cerevisiae*. *Eukaryot Cell* **6:** 1150–1165.

Lim, J.Y., Park, Y.H., Pyon, Y.H., Yang, J.M., Yoon, J.Y., Park, S.J., *et al*. (2020) The LAMMER kinase is involved in morphogenesis and response to cell wall- and DNA-damaging stresses in *Candida albicans*. *Med Mycol* **58:** 240–247.

Liu, N.N., Flanagan, P.R., Zeng, J., Jani, N.M., Cardenas, M.E., Moran, G.P., and Köhler, J.R. (2017) Phosphate is

the third nutrient monitored by TOR in *Candida albicans* and provides a target for fungal-specific indirect TOR inhibition. *Proc Natl Acad Sci USA* **114:** 6346–6351.

Livak, K.J., and Schmittgen, T.D. (2001) Analysis of relative gene expression data using real-time quantitative PCR and the 2(-Delta Delta C(T)) Method. *Methods (San Diego, Calif.)* **25:** 402–408.

Maesaki, S., Marichal, P., Vanden Bossche, H., Sanglard, D., and Kohno, S. (1999) Rhodamine 6G efflux for the detection of CDR1-overexpressing azole-resistant *Candida albicans* strains. *J Antimicrob Chemother* **44:** 27–31.

Martínez-Muñoz, G.A., and Kane, P. (2017) Vacuolar and plasma membrane proton pumps collaborate to achieve cytosolic pH homeostasis in yeast. *J Biol Chem* **292:** 7743.

Mei, Y., Jiang, T., Zou, Y., Wang, Y., Zhou, J., Li, J., *et al*. (2020) FDA approved drug library screening identifies robenidine as a repositionable antifungal. *Front Microbiol* **11:** 996.

Mishra, N.N., Prasad, T., Sharma, N., Payasi, A., Prasad, R., Gupta, D.K., and Singh, R. (2007) Pathogenicity and drug resistance in *Candida albicans* and other yeast species. A review. *Acta microbiologica et immunologica Hungarica* **54:** 201–235.

Mitchell, P. (2011) Chemiosmotic coupling in oxidative and photosynthetic phosphorylation. 1966. *Biochem Biophys Acta* **1807:** 1507–1538.

Mitchell, R., Hopcroft, L.E.M., Baquero, P., Allan, E.K., Hewit, K., James, D., *et al*. (2018) Targeting BCR-ABL-independent TKI resistance in chronic myeloid leukemia by mTOR and autophagy inhibition. *J Natl Cancer Inst* **110:** 467–478.

Monk, B.C., Kurtz, M.B., Marrinan, J.A., and Perlin, D.S. (1991) Cloning and characterization of the plasma membrane H(+)-ATPase from *Candida albicans*. *J Bacteriol* **173:** 6826–6836.

Monk, B.C., Mason, A.B., Kardos, T.B., and Perlin, D.S. (1995) Targeting the fungal plasma membrane proton pump. *Acta Biochim Pol* **42:** 481–496.

Monk, B.C., Niimi, K., Lin, S., Knight, A., Kardos, T.B., Cannon, R.D., *et al*. (2005) Surface-active fungicidal D-peptide inhibitors of the plasma membrane proton pump that block azole resistance. *Antimicrob Agents Chemother* **49:** 57–70.

Musumeci, F., Greco, C., Grossi, G., Molinari, A., and Schenone, S. (2018) Recent studies on ponatinib in cancers other than chronic myeloid leukemia. *Cancers* **10:** 430.

Nakamura, K., Niimi, M., Niimi, K., Holmes, A.R., Yates, J.E., Decottignies, A., *et al*. (2001) Functional expression of *Candida albicans* drug efflux pump Cdr1p in a *Saccharomyces cerevisiae* strain deficient in membrane transporters. *Antimicrob Agents Chemother* **45:** 3366–3374.

Odds, F.C. (2003) Synergy, antagonism, and what the chequerboard puts between them. *J Antimicrob Chemother* **52:** 1.

Ohgaki, R., van, I. S. C. Matsushita, M., Hoekstra, D., and Kanazawa, H. (2011) Organellar Na+/H+ exchangers: novel players in organelle pH regulation and their emerging functions. *Biochemistry* **50:** 443–450.

Orij, R., Brul, S., and Smits, G.J. (2011) Intracellular pH is a tightly controlled signal in yeast. *Biochem Biophys Acta* **1810:** 933–944.

Ottilie, S., Goldgof, G.M., Cheung, A.L., Walker, J.L., Vigil, E., Allen, K.E., *et al*. (2018) Two inhibitors of yeast plasma membrane ATPase 1 (ScPma1p): toward the development of novel antifungal therapies. *J Cheminform* **10:** 6.

Perlin, D.S., Seto-Young, D., and Monk, B.C. (1997) The plasma membrane H(+)-ATPase of fungi. A candidate drug target? *Ann N Y Acad Sci* **834:** 609–617.

Poznanski, J., Szczesny, P., Ruszczyńska, K., Zielenkiewicz, P., and Paczek, L. (2013) Proteins contribute insignificantly to the intrinsic buffering capacity of yeast cytoplasm. *Biochem Biophys Res Comm* **430:** 741–744.

Prasad, R., and Goffeau, A. (2012) Yeast ATP-binding cassette transporters conferring multidrug resistance. *Annu Rev Microbiol* **66:** 39–63.

Rand, K.H., Houck, H.J., Brown, P., and Bennett, D. (1993) Reproducibility of the microdilution checkerboard method for antibiotic synergy. *Antimicrob Agents Chemother* **37:** 613–615.

Rex, J.H. (2008) *Reference Method for Broth Dilution Antifungal Susceptibility Testing of Yeasts*. Approved Standard M27-A3, Clinical and Laboratory Standards Institute.

Robbins, N., Spitzer, M., Yu, T., Cerone, R.P., Averette, A.K., Bahn, Y.-S., *et al*. (2015) An antifungal combination matrix identifies a rich pool of adjuvant molecules that enhance drug activity against diverse fungal pathogens. *Cell Rep* **13:** 1481–1492.

Ruggero, M.A., and Topal, J.E. (2014) Development of echinocandin-resistant *Candida albicans* candidemia following brief prophylactic exposure to micafungin therapy. *Transpl infect Dis* **16:** 469–472.

Saliba, E., Evangelinos, M., Gournas, C., Corrillon, F., Georis, I., and André, B. (2018) The yeast H+-ATPase Pma1 promotes Rag/Gtr-dependent TORC1 activation in response to H+-coupled nutrient uptake. *eLife* **7:** e31981. https://doi.org/10.7554/eLife.31981

Serrano, R. (1988) Structure and function of proton translocating ATPase in plasma membranes of plants and fungi. *Biochem Biophys Acta* **947:** 1–28.

Shapiro, R.S., Robbins, N., and Cowen, L.E. (2011) Regulatory circuitry governing fungal development, drug resistance, and disease. *Microbiol Mol Biol Rev* **75:** 213–267.

Shekhar-Guturja, T., Gunaherath, G.M.K.B., Wijeratne, E.M.K., Lambert, J.-P., Averette, A.F., Lee, S.C., *et al*. (2016a) Dual action antifungal small molecule modulates multidrug efflux and TOR signaling. *Nat Chem Biol* **12:** 867–875.

Shekhar-Guturja, T., Tebung, W.A., Mount, H., Liu, N., Köhler, J.R., Whiteway, M., and Cowen, L.E. (2016b) Beauvericin potentiates azole activity via inhibition of multidrug efflux, blocks *Candida albicans* Morphogenesis, and is effluxed via Yor1 and circuitry controlled by Zcf29. *Antimicrob Agents Chemother* **60:** 7468–7480.

Spitzer, M., Griffiths, E., Blakely, K.M., Wildenhain, J., Ejim, L., Rossi, L., *et al*. (2011) Cross-species discovery of syncretic drug combinations that potentiate the antifungal fluconazole. *Mol Syst Biol* **7:** 499.

Stewart, E., Gow, N.A., and Bowen, D.V. (1988) Cytoplasmic alkalinization during germ tube formation in *Candida albicans*. *J Gen Microbiol* **134:** 1079–1087.

Sukheja, P., Kumar, P., Mittal, N., Li, S. G., Singleton, E., and Russo, R., *et al*. (2017) A novel small-molecule inhibitor of the mycobacterium tuberculosis demethylmenaquinone methyltransferase MenG is bactericidal to both growing and nutritionally deprived persister cells. *mBio* **8:** e02022–16. https://doi.org/10.1128/mBio.02022-16.

Suzuki, Y.o., Onge, R.P.S., Mani, R., King, O.D., Heilbut, A., Labunskyy, V.M., *et al*. (2011) Knocking out multigene redundancies via cycles of sexual assortment and fluorescence selection. *Nat Methods* **8:** 159–164.

Toenjes, K.A., Munsee, S.M., Ibrahim, A.S., Jeffrey, R., Edwards, J.E. Jr, and Johnson, D.I. (2005) Small-molecule inhibitors of the budded-to-hyphal-form transition in the pathogenic yeast *Candida albicans*. *Antimicrob Agents Chemother* **49:** 963–972.

van der Rest, M.E., Kamminga, A.H., Nakano, A., Anraku, Y., Poolman, B., and Konings, W.N. (1995) The plasma membrane of *Saccharomyces cerevisiae*: structure, function, and biogenesis. *Microbiol Rev* **59:** 304–322.

Van Dyke, R.W., Hornick, C.A., Belcher, J., Scharschmidt, B.F., and Havel, R.J. (1985) Identification and characterization of ATP-dependent proton transport by rat liver multivesicular bodies. *J Biol Chem* **260:** 11021–11026.

Vincent, B.M., Langlois, J.B., Srinivas, R., Lancaster, A.K., Scherz-Shouval, R., Whitesell, L., *et al*. (2016) A fungal-selective cytochrome bc(1) inhibitor impairs virulence and prevents the evolution of drug resistance. *Cell Chem Biol* **23:** 978–991.

Wang, J., Ye, X., Yang, X., Cai, Y., Wang, S., Tang, J., *et al*. (2020) Discovery of novel antibiotics as covalent inhibitors of fatty acid synthesis. *ACS Chem Biol* **15:** 1826–1834.

Witchley, J.N., Penumetcha, P., Abon, N.V., Woolford, C.A., Mitchell, A.P., and Noble, S.M. (2019) *Candida albicans* morphogenesis programs control the balance between gut commensalism and invasive infection. *Cell Host Microbe* **25:** 432–443.e436.

Xu, H., Whiteway, M., and Jiang, L. (2019) The tricarboxylic acid cycle, cell wall integrity pathway, cytokinesis and intracellular pH homeostasis are involved in the sensitivity of *Candida albicans* cells to high levels of extracellular calcium. *Genomics* **111:** 1226–1230.

Yang, H., Tsang, P.C.S., Pow, E.H.N., Lam, O.L.T., and Tsang, P.W. (2020) Potential role of *Candida albicans* secreted aspartic protease 9 in serum induced-hyphal formation and interaction with oral epithelial cells. *Microb Pathog* **139:** 103896.

Zhang, Y.Q., Gamarra, S., Garcia-Effron, G., Park, S., Perlin, D.S., and Rao, R. (2010) Requirement for ergosterol in V-ATPase function underlies antifungal activity of azole drugs. *PLoS Pathog* **6:** e1000939.

Supporting information

Additional supporting information may be found online in the Supporting Information section at the end of the article.

Fig. S1. Combination of ponatinib and fluconazole synergistically inhibits growth of *C. albicans*. *C. albicans* (SC5314) was subjected to 4 μM ponatinib combined with two-fold serial dilutions of fluconazole in YPD medium. OD_{600} was measured every 15 min at 30°C.

Fig. S2. Ponatinib is non-toxic at 16 μM or lower by lactate dehydrogenase assay. Endothelial cells (NCM460) were exposed to two-fold serial dilutions of ponatinib in DMEM at 37°C for 1.5 h.

Fig. S3. The visible MIC of fluconazole or ponatinib on *C. albicans*, *S. cerevisiae*, *C. neoformans* and fluconazole-resistant clinical *C. albicans* isolates. (A) Two-fold serial dilutions of fluconazole or ponatinib in YPD without fungi. (B) *C. albicans* was exposed to two-fold serial dilutions of fluconazole or ponatinib in YPD. (C) *S. cerevisiae* was exposed to two-fold serial dilutions of fluconazole or ponatinib in YPD. (D) *C. neoformans* was exposed to two-fold serial dilutions of fluconazole or ponatinib in YPD. (E) Fluconazole-resistant clinical *C. albicans* isolates (CCC49) was exposed to two-fold serial dilutions of fluconazole or ponatinib in YPD. (F) Fluconazole-resistant clinical *C. albicans* isolates (CCC80) was exposed to two-fold serial dilutions of fluconazole or ponatinib in YPD. The plates of *C. albicans*, *S. cerevisiae* and fluconazole-resistant clinical *C. albicans* isolates were incubated at 30°C for 24h, the plate of *C. neoformans* was incubated at 30°C for 72h and all the plates were photographed by ChemiDoc MP (Bio-Rad).

Fig. S4. Transcriptional expression of *PDR5* in *S. cerevisiae* was quantified under treatment with ponatinib. Cells were subjected to DMSO or ponatinib in YPD at 30°C for 4 h. Experiments were performed in biological triplicates.

Fig. S5. The proton pump in the membrane was enhanced by fluconazole but inhibited when combined with ponatinib. IOV (In-side out) of 4741 was subjected to DMSO, N-ethylmaleimide (NEM) (10 μM) + Orthovanadate (OV) (100 μM), fluconazole (16 μg ml^{-1}), ponatinib (8 μM) or fluconazole (16 μg ml^{-1}) + ponatinib (8 μM) for 1 h. Experiments were performed in biological triplicates.

